Diffraction on birefringent elements with sine surface microrelief

V. V. Belyaev (SID Member)
V. M. Novikovich
P. L. Denisenko

Abstract — Light diffraction on optically anisotropic substrates using sine surface microrelief has been calculated by using the OAGSM method. The influence of the microrelief depth and material birefringence on the diffraction intensity on the order of 0–3 is reviewed and discussed. The results are compared with the results of the calculation for a rectangular microrelief. The microrelief depth and material birefringence allows the realization of different polarization states of the light beam transmitted or reflected by the substrate. The approach can be used to control the light-beam propagation for different applications including LCD backlights.

Keywords — *??*

1 Introduction

Many recent LCD, LED, and OLED arrays have compone nts with surface microrelief to enhance the light efficiency of the device,[1,2] *e.g.*, such diffractive components were proposed for backlighting the LCDs used in mobile phones.[3,4] The microrelief has various periodicities and different shapes (sine, triangle, rectangular, cylinder, *etc*.). As a rule, optically isotropic materials are used for these components. Some methods of calculation of the optical properties of such gratings are described in Refs. 5 and 6. Utilization of only isotropic media in such components implies some restrictions on the modification of LCD performance for their improvement.

For LCDs where their main component has a microrelief that is a light-guide plate (LGP) or light-outcoupling elements on the LGP surface. There are not many applications of birefringent materials in these elements.[7–9] It is especially difficult to model polarized light propagation in them in the absence of a reliable and fast method for such calculations.

In Refs. 10–12, the Optical Anisotropic Gratings with Surface Microrelief (OAGSM) approach was developed to calculate polarized light diffraction in birefringent media with surface microrelief. The advantages of this method are as follows: calculation of new diffraction optical elements (DOEs) with simple functions of separation and/or deflection of light beam independently on its polarization as well as with a combination of these functions having different polarizations. Besides this, the method provides a short calculation time compared with other software.

In Ref. 12, this approach was checked for gratings with rectangular microrelief. The goal of the paper is to implement such calculations for the case of sine microrelief and compare them with the results for rectangular microrelief. The method and the results obtained can be used for the development of new optical polarizing elements.

2 Calculation parameters

Figure 1 illustrates the calculation parameters. A substrate has a solid part with thickness H and a microrelief part. The periodical sinusoidal or rectangular microrelief is characterized by the period Λ and depth h (both Λ and h are normalized to the light-beam wavelength λ). The material of the substrate is a uniaxial medium (a polymer or a liquid crystal) with the largest refraction index ($n_e = n_2$) in the direction of the grooves. For comparison, the case of the isotropic material ($n_1 = n_2 = n_3 = 1.50$) was also considered too.

In our calculations, the solid part was absent ($H = 0$). The incidence angle of a light beam with respect to the substrate normal is designated as θ. In our paper, only the case of the normal incidence is considered. The vector of the polarization is revolved by the angle $\varphi = 45°$ relative to the direction of the grooves of the microrelief. It has two components – *TE* and *TM* – that are perpendicular and parallel to the grooves, respectively.

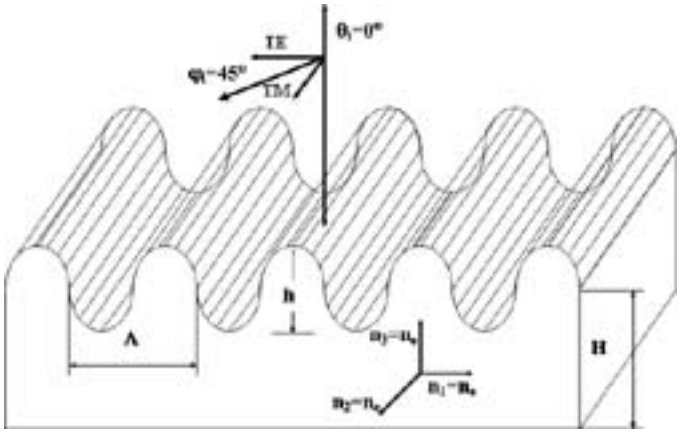

FIGURE 1 — Geometrical dimensions of a microreliefed substrate (H – thickness, Λ – microrelief period, h – microrelief height); its optical axis and *TM* wave are parallel to the grooves; *TE* wave is perpendicular to the grooves.

Extended revised version of a paper presented at EuroDisplay 2007 held September 17–20, 2007 in Moscow, Russia.

V. V. Belyaev is with the Kurchatov Institute, Agency for Biomedical Technologies and Nuclear Medicine, 1 Kurchatov Sq., Moscow, 123182 Russia; telephone +7-495-577-1981, fax +7-499-196-6943, e-mail: vic_belyaev@mail.ru.

V. M. Novikovich and P. L. Denisenko are with the Moscow Region State University, Moscow, Russia.

The computations were made for the sinusoidal microrelief and the results were compared with the results obtained for the rectangular microrelief.[11,12] The refraction-index value for an ordinary ray was assigned equal to 1.50 and for the extraordinary ray 1.50, 1.55, 1.60, and 1.70, respectively.

3 Calculation results

Let us review first the thickness dependencies of the diffraction intensity on the orders from zero to three in accordance with the components of both transmitted and reflected *TE* and *TM* waves, respectively (Fig. 2).

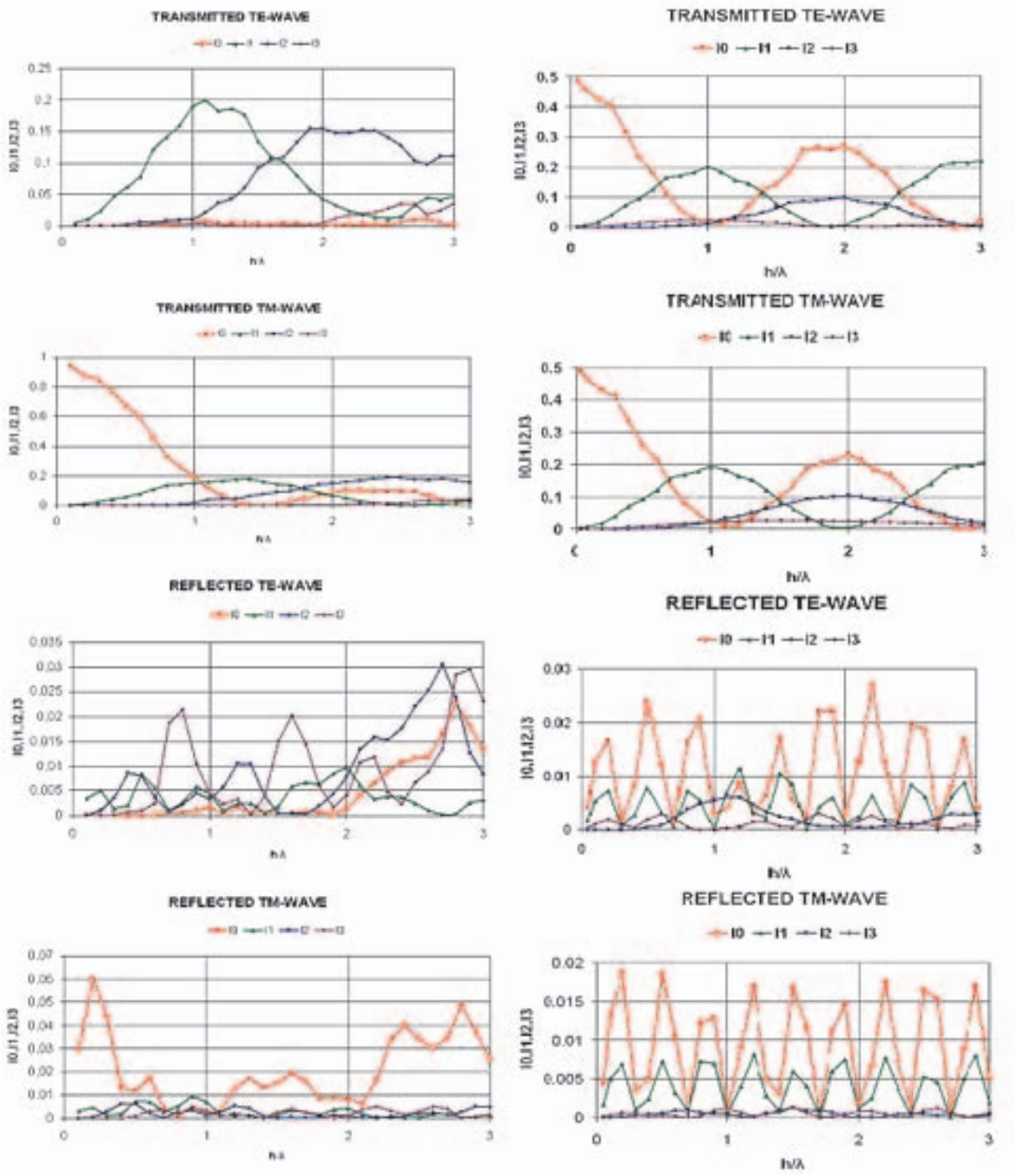

FIGURE 2 — Results of the calculation of the intensities of the diffraction orders 0, 1, 2, and 3 for both transmitted and reflected *TE* and *TM* waves. Left – sine and right – rectangular microrelief. $\Delta n = 0$; $n_1 = n_3 = 1.5$.

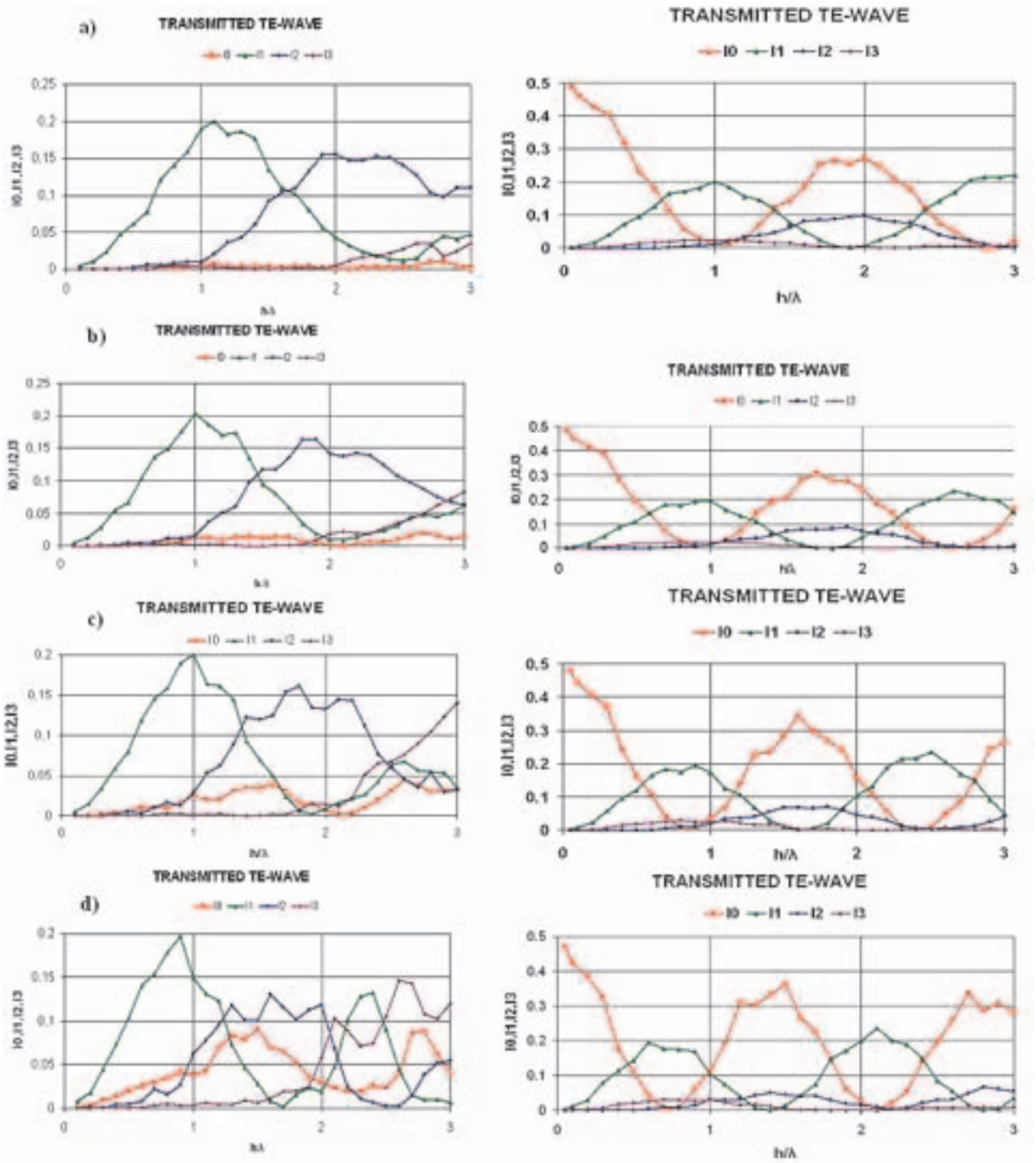

FIGURE 3 — Dependency of the diffraction efficiency in the zero, first, second, and third diffraction orders of the transmitted *TE* wave *vs.* the microrelief depth reduced to the wavelength for both sine (left) and rectangular (right) microrelief at a substrate birefringence Δn = 0 (a), 0.05 (b), 0.1 (c), 0.2 (d). $n_1 = n_3 = 1.5$.

In general, the intensity of the transmitted *TE* and *TM* waves considerably exceeds the intensity of the corresponding reflected waves. For the rectangular microrelief, the calculated intensity of the reflected *TE* and *TM* waves does not exceed the value of 0.03, and for the sinusoidal microrelief, it is less than 0.07.

The apparent periodicity of the I_0 and I_1 dependencies on the thickness for the reflected waves is most likely a result of the calculation inaccuracy. Dispersion of the calculated I_0 and I_1 values for both transmitted *TE* and *TM* waves is approximately on the same order.

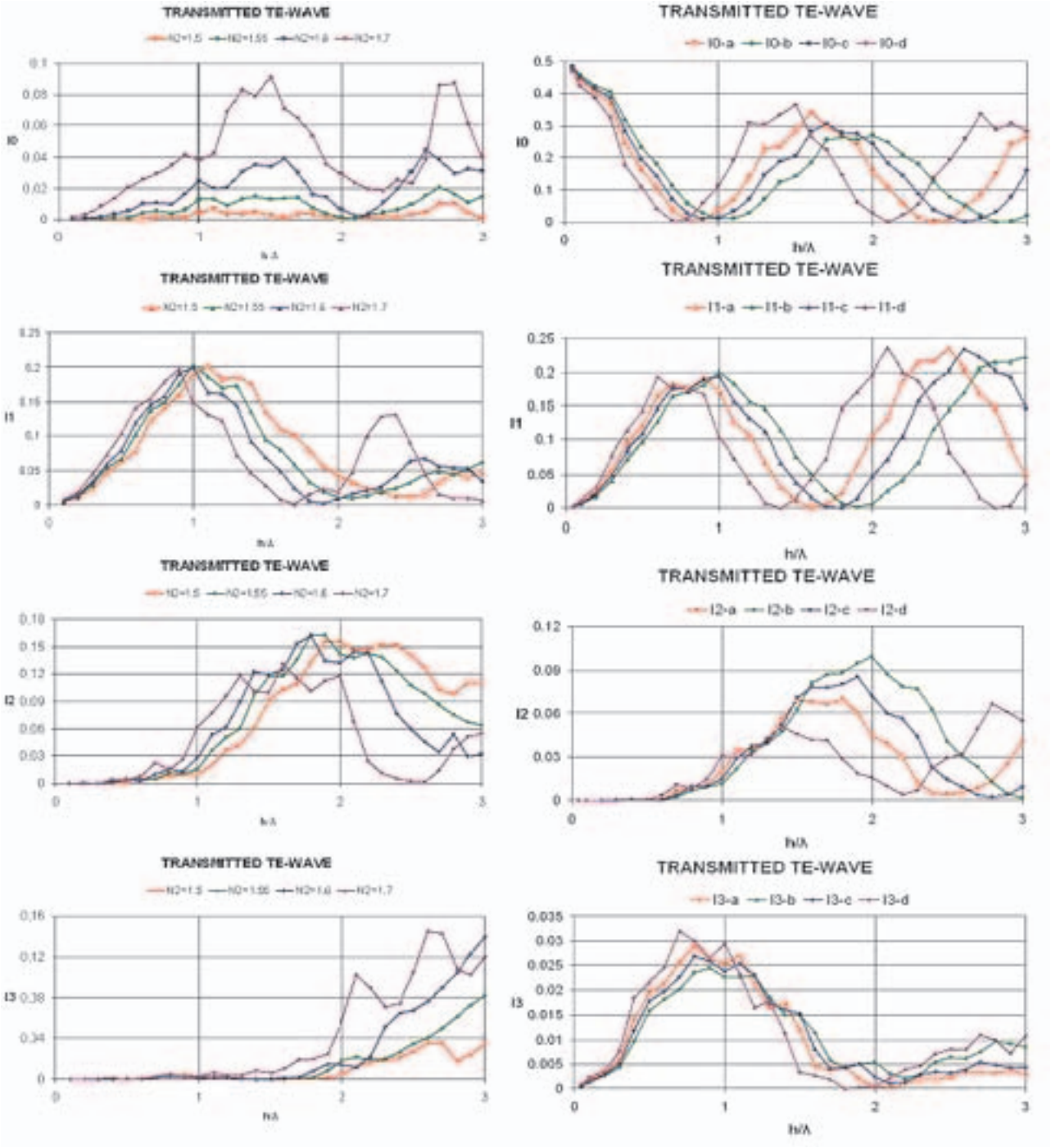

FIGURE 4 — Comparison of the dependency of the diffraction efficiency in the the zero, first, second, and third diffraction orders of the transmitted *TE* wave *vs.* the microrelief depth reduced to the wavelength at different values of the substrate birefringence for both sine (left) and rectangular (right) microrelief. (a) $\Delta n = 0$; (b) $\Delta n = 0.05$; (c) $\Delta n = 0.1$; (d) $\Delta n = 0.2$. $n_1 = n_3 = 1.5$.

Therefore, the main attention is paid to the dependencies of the diffraction intensity on the thickness for only transmitted *TE* and *TM* waves.

The dependencies of the $I_0 - I_3$ diffraction order intensity on h/λ for both transmitted *TE* and *TM* waves at different birefringence values are shown in Fig. 3. Let us note the main distinctions of these dependences for both the sinusoidal and rectangular microrelief.

The dependencies $I_0(h/\lambda) - I_3(h/\lambda)$ have an oscillating form with a relative height with maximums that are approximately equal to $I_0^{TE} = 0.5$, $I_1^{TE} = 0.2$, $I_2^{TE} = 0.1$, $I_3^{TE} = 0.03$ for the rectangular microrelief and $I_1^{TE} = 0.2$, $I_2^{TE} = 0.17$, $I_3^{TE} = 0.07$ for the sinusoidal microrelief. The maxima location depends on Δn (see Fig. 4 and a corresponding text). In the case of the sinusoidal microrelief, the I_2^{TE} and I_3^{TE} values are about twice as high as corresponding values

for the rectangular microrelief, and the shape of the $I_0^{TE}(h/\lambda)$ dependence is essentially changed.

For the rectangular microrelief, both maxima and minima of the I_0^{TE} and I_1^{TE} dependencies are in the antiphase, *i.e.*, the location of the $I_0(h/\lambda)$ minima corresponds to the location of the $I_1(h/\lambda)$ maxima and vice versa. When the Δn value increases then the position of the extrema for both dependences shifts equally (see below). For the sinusoidal microrelief, the location of the maxima for the $I_0(h/\lambda)$ dependency does not correspond to the location of the minima in the $I_1(h/\lambda)$ dependency.

As for $I_2^{TE}(h/\lambda)$ dependencies, for the rectangular microrelief, the location of their maximum corresponds to the location of the second maximum of the $I_0(h/\lambda)$ curve and the first minimum of the $I_1(h/\lambda)$ dependency, while for the sinusoidal microrelief the location of the $I_2^{TE}(h/\lambda)$ maximum corresponds to the location of the first minimum of the $I_1(h/\lambda)$ dependency.

For the $I_3^{TE}(h/\lambda)$ dependencies, the location of their first maximum corresponds approximately to the location of the first minimum of the $I_1(h/\lambda)$ dependency. The maximum height is very low, it is comparable to the calculation accuracy. For the sinusoidal microrelief, the $I_3^{TE}(h/\lambda)$ value is almost zero for $h/\lambda \le 1.5$, then it increases to $I_3 = 0.05$ ($\Delta n = 0$) and $I_3 = 0.15$ ($\Delta n = 0.2$) at $h/\lambda = 3$.

The influence of the birefringence Δn on the location of the $I_0^{TE} - I_3^{TE}$ extrema and their values is shown in Fig. 4 with separate thickness dependencies for each diffraction order at different Δn values.

For diffraction on the rectangular microrelief, the location of the first minimum for the zeroth-order shifts to a lower thickness with the birefringence growth: from $h/\lambda = 1.0$ at $\Delta n = 0$ up to $h/\lambda = 0.75$ at $\Delta n = 0.2$. The same is true for other extrema. The intensity of the next maximum increases by 30% at the Δn growth from 0 to 0.2. For the sinusoidal microrelief, the shift of the maximum I_0^{TE} is small, but the intensity value increases essentially with the

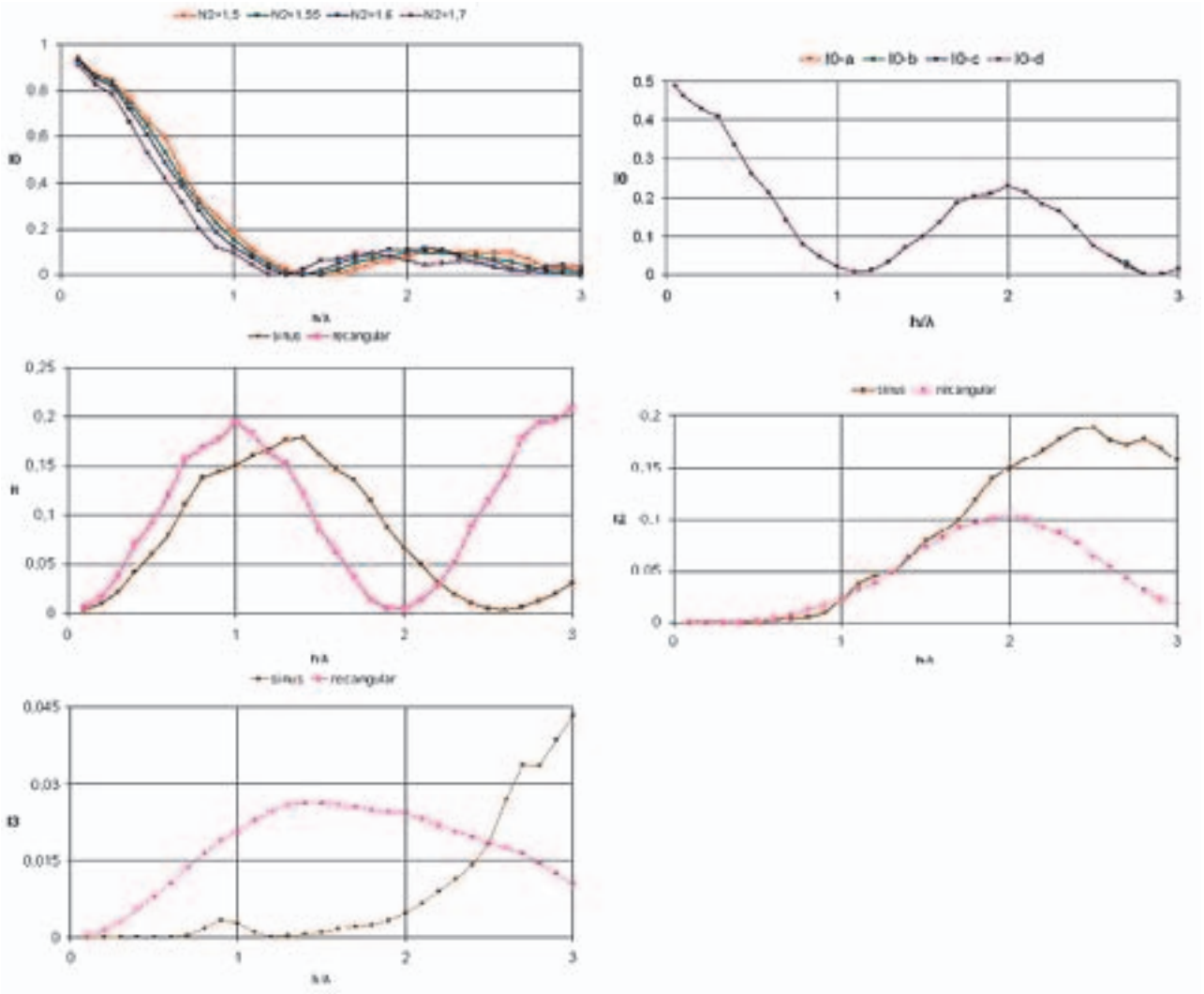

FIGURE 5 — Dependence of the diffraction efficiency in the zero, first, second, and third diffraction orders of the transmitted *TM* wave *vs.* the microrelief depth reduced to the wavelength for both sine and rectangular microrelief. I_0^{TM} – left – sine and right – rectangular microrelief. n_2 values are in the legend. All curves for the rectangular microrelief at different Δn are overlapped.

Δn growth owing to the longer optical path for extraordinary waves.

For the first order (rectangular microrelief), the shift of the extrema location is similar to the one described for the zeroth order, and the intensity of the second maximum increases by 10% in comparison with the first maximum. For both maxima, their intensity does not depend on the Δn value. For the sinusoidal microrelief, the location of the first maximum and its intensity corresponds to the same value for the rectangular microrelief. However, the location of other extrema is observed at essentially higher h/λ values than in the case of the rectangular microrelief. The height of the second maximum is 1.5 times lower than the height of the first maximum. A characteristic property of the diffraction on the sinusoidal microrelief is the non-zero intensity at the first minimum at low Δn values.

For the second order (rectangular microrelief), the shift of the first maximum location to lower thickness is also observed (from $h/\lambda = 2.0$ at $\Delta n = 0$ to $h/\lambda = 1.4$ at $\Delta n = 0.2$). The maximum's intensity is reduced 2× for a Δn change from 0 to 0.2. Similar behavior is observed for the corresponding dependencies for the sinusoidal microrelief (the shift of the first maximum from $h/\lambda = 2.2$ at $\Delta n = 0$ to $h/\lambda = 1.6$ at $\Delta n = 0.2$ and small reduction in intensity).

For the third order, it is difficult to judge the maximum's shift and a change in its intensity owing to insufficient calculation accuracy for the rectangular microrelief. For the sinusoidal microrelief, the I_3 value increases with the Δn growth.

Let us compare the thickness dependencies of the intensities for both polarization types (*TE* and *TM* waves) and both microrelief types (Fig. 5) and point to the essential distinctions. If, for the rectangular microrelief, both I_0^{TM} and I_0^{TE} ($\Delta n = 0$) dependences are identical and I_0^{TM} does not depend on Δn, then the I_0^{TM} and I_0^{TE} dependencies for the sine microrelief strikingly differ. For the rectangular microrelief, there is a correlation between the locations of the I_0^{TM}, I_1^{TM}, and I_2^{TM} features. For the sinusoidal microrelief, the I_0^{TM} dependency has its first minimum at $h/\lambda = 1.1$, and the I_1^{TM} dependency has its first maximum at $h/\lambda = 1.25$. The locations of the I_1^{TM} minimum and the I_2^{TM} maximum coincide ($h/\lambda = 2.4$). The I_3^{TM} dependency has n on-zero values only at $h/\lambda > 2$.

Application of the OAGSM software allows for different combinations of both *TE* and *TM* waves in the diffraction orders. Some examples of such combinations are presented in Figs. 6 and 7. In Fig. 6, an opportunity to suppress both *TE* and *TM* waves or only *TE*-wave polarizations in the zero order and transmission of both positive and negative first orders for both polarizations is shown for a normally incident beam.

In Fig. 7, a case of a tilted incident beam is shown. Parameters of the grating are selected in such a way that for the *TE* wave the grating functions as a splitter, and for the *TM* wave as a deflector. At the grating output, the zero beam has a linear polarization, but the first beam has an elliptical polarization.

Some other cases of beam splitting or deflection for both rectangular and sine microrelief were described in Ref. 11.

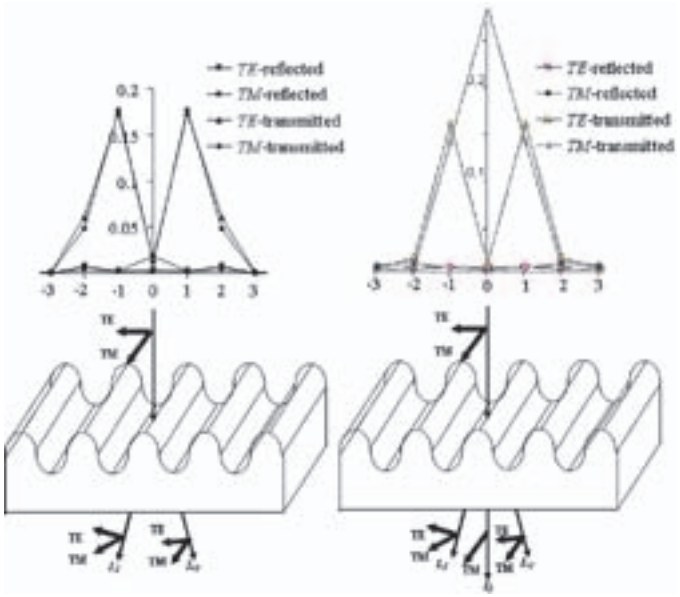

FIGURE 6 — Left: suppression of both *TE* and *TM* polarizations in the zero order and transmission of both positive and negative first orders for both polarizations in the sine microrelief grating with $n_o = 1.50$, $n_e = 1.55$, $h/\lambda = 1.3$. Right: suppression of only *TE* polarization in the zero order and transmission of both positive and negative first orders for both polarizations in the sine microrelief grating with $n_o = 1.50$, $n_e = 1.6$, $h/\lambda = 0.8$. Normal incidence ($\theta = 0°$).

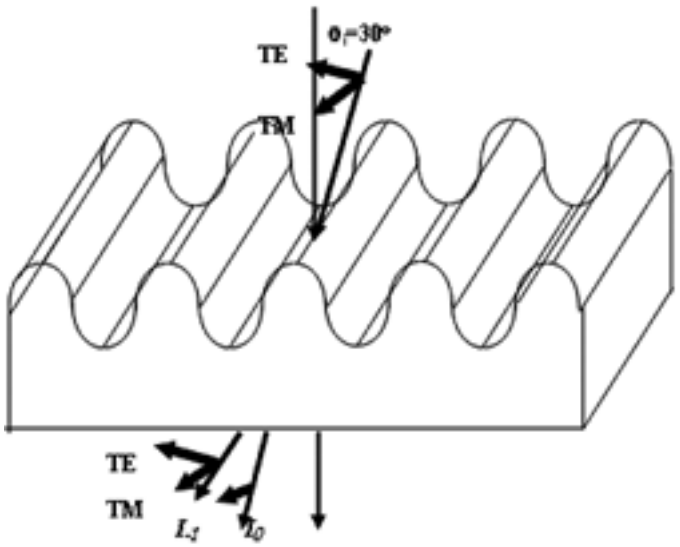

FIGURE 7 — Incidence of a tilted beam ($\theta = 30°$) onto a sine grating with parameters $h/\lambda = 1.95$, $H/\lambda = 2.5$, $\Lambda/\lambda = 1$, $n_o = 1.5$, $n_e = 1.777$. For the *TE* wave the grating works as a splitter, and for the *TM* wave it works as a deflector. The zero beam has a linear polarization, and the first beam has an elliptical polarization.

4 Conclusion

The presence of birefringence in the sinusoidal gratings with microrelief results in essential changes of the I_0^{TE}, I_0^{TM}, and I_1^{TE} dependencies on thickness. The birefringence influences the extrema locations of the $I_0^{TE} - I_3^{TE}$ dependencies and their intensities.

That is important for many practical applications. It is obvious that by varying the microrelief parameters (depth and period) as well as refractive indices of the anisotropic medium with surface microrelief results in a realization of almost any combination of *TE* and *TM* waves, *i.e.*, almost any polarization state of the light beam transmitted or reflected by the substrate. Additionally, by varying the microrelief shape, one can achieve better homogeneity of an LCD backlight.[1,2] Modeling of the LCD backlight with birefringent elements having optical anisotropy requires working with a wide range of wavelength and incidence angles as well as material parameters: birefringence and microrelief shape, height, and depth. This work is planned in future.

Acknowledgments

This work was supported in part by the Russian Foundation for Basic Researches, grant #06-03-81035-Bel_a.

The authors thank Ms. E. Kushnir for her assistance in the calculations.

References

1 C.-Y. Kim and T.-H. Choi, *Proc. IDMC '02*, 185 (2002).
2 U.S. Patent 6,791,636 Lumileds Lighting (2005).
3 J. Kimmel, T. Levola, and P. Laakkonen, "Diffractive backlight grating array for mobile displays," *J Soc. Info. Display* **16**, No. 9, 863–870 (2008).
4 M. J. J. Jak, R. Caputo, E. J. Hornix, L. de Sio, D. K. G. de Boer, and H. J. Cornelissen, "Colour separating backlight for improved LCD efficiency," *Proc. EuroDisplay '07*, 18–20 (2007).
5 C. Oh, R. Komanduri, and M. J. Escuti, "FDTD and elastic continuum analysis of the liquid crystal polarization grating," *SID Symposium Digest Tech. Papers* **37**, 844–847 (2006).
6 L. Doskolovich, E. Tyavin, N. Kazanskii, and O. Petrova, "Calculation and research of color separating diffraction gratings," *Computer Opt.*, No. 27, 11–16 (2005).
7 U.S. Patent 7331682, "Back light module with birefringent crystal assemblies."
8 K.-W. Chien, H.-P. D. Shieh, and H. Cornelissen, "Polarized backlight based on selective total internal reflection at microgrooves," *Appl. Opt.* **43**, 4672–4676 (2004).
9 WO Patent Application 2006/031545 2006032.3.
10 V. Tsoy, V. Belyaev, V. Misnik, D. Litovchenko, and A. Tarasishin, "Simulation of light propagation through birefringent substrates with periodical surface microrelief," *Opt. Commun.* **246**, 57–66 (2005).
11 V. V. Belyaev, V. I. Tsoy, E. M. Kushnir, A. V. Klyckov, and A. Y. Kalashnikov, "Polarized light diffraction on anisotropic substrates with rectangular and sine microrelief," *J Soc. Info. Display* **13**, 305–308 (2005).
12 V. V. Belyaev, E. M. Kushnir, A. V. Klyckov, and V. I. Tsoy, "Numerical simulation of light diffraction on periodical anisotropic gratings with surface rectangular microrelief," *J. Opt. Technol.* **72**, 86–90 (2005).

Victor Belyaev, D.Sc., Honorary Director of SID Russia Chapter graduated from Moscow Institute for Physics and Technology (MIPT) in 1974. In 1980, he defended his Ph.D. thesis entitled, "Investigations of orientation electro-optic effects in liquid crystals." In 1996, he defended his D.Sc. (hab.) thesis entitled "Liquid crystals in optical systems for information transformation and displaying." Currently, he holds a position of Head of Agency in Russian Research Centre "Kurchatov Institute." His scientific interests include material sciences and electronics, display devices, systems and technologies, problems of physics and application of liquid crystals and polymer materials, information technologies, investigation of display market, visual perception, image processing, bio-medicine technologies, and nuclear medicine.

Vadim M. Novikovich graduated from the University in 1959 as an electrician–engineer. He has been engineer–programmer since 1963. In 1973, he defended his Ph.D. thesis. Since 1977, he has been Superior Science Researcher. Dr. Novikovich has been Chief of Science Research Department of Moscow State Regional University since 1996. His specialty is system analysis, management, and data processing.

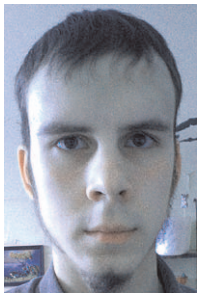

Peter L. Denisenko graduated from Moscow Region State University in 2007, specialty in physics and computer science. At present, he is a post-graduated student of this university. He has been Secretary of Science Research Department of Moscow Region State University since 2007.